Reaction Kinetics, Mechanisms and Catalysis (2022) 135:2441–2455
https://doi.org/10.1007/s11144-022-02255-1

Performance and kinetics of silicon-bridged diphosphines/$CrCl_3(C_4H_8O)_3$/modified methylaluminoxane catalyzed ethylene tri-/tetramerization in a continuous stirred tank reactor

Xun Wang[1] · **Yating Wang**[1] · **Jing Ma**[1] · **Qihuan He**[1] · **Huaiqi Shao**[1] · **Yongrui Li**[1] · **Jingyi Zhang**[1] · **Qian Zhang**[1] · **Qian Liu**[1] · **Tao Jiang**[1]

Received: 16 May 2022 / Accepted: 23 June 2022 / Published online: 16 July 2022

Abstract

In this study, PNSiP, a silicon-bridged diphosphines ligand, was coupled with $CrCl_3(THF)_3$ and modified methylaluminoxane (MMAO) to form a catalytic system. The continuous ethylene tri-/tetramerization catalytic performance of the PNSiP/$CrCl_3(THF)_3$/MMAO system was evaluated with a self-designed continuous stirred tank reactor (CSTR). The products have more than 88.00% selectivity for 1-hexene and 1-octene. Cyclic-C_6 by-products (methyl-cyclopentane and methylene-cyclopentane) have a selectivity of less than 1.00%. The optimal process parameters for continuous ethylene tri-/tetramerization in CSTR were 60 °C reaction temperature, 5.0 MPa ethylene pressure, 1.2 mL/min catalyst feed flow rate, and 200 r/min impeller speed. The catalytic activity of the system can reach 7.26×10^5 g(products) $g(Cr)^{-1}$ h^{-1}. The mass fraction of polyethylene is less than 0.15% after 30 h. Finally, a kinetic model was established to describe the effects of chromium concentration and ethylene pressure on the continuous reaction of PNSiP/$CrCl_3(THF)_3$/MMAO catalyzed ethylene tri-/tetramerization in CSTR under the optimum conditions. This paper provides data basis and preliminary preparation for the continuous industrial production of linear α-olefins.

Xun Wang and Yating Wang have contributed equally to this work.

✉ Tao Jiang
jiangtao@tust.edu.cn

[1] College of Chemical Engineering and Material Science, Tianjin University of Science and Technology, Tianjin 300457, China

Graphical abstract

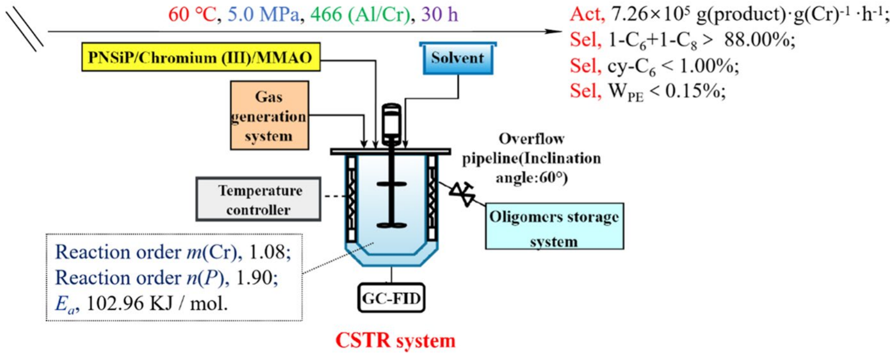

Keywords Diphosphines/chromium complex · Linear α-olefins · Ethylene tri-/tetramerization · Kinetics · Continuous stirred tank reactor

Introduction

Linear α-olefins (LAOs), primarily 1-hexene and 1-octene, have a low energy consumption and high market demand, making them suitable for utilization as raw materials in polyolefin comonomers [1, 2]. Non-selective ethylene oligomerization produces LAOs with the Schulz–Flory distribution or the Poisson distribution, resulting in difficult product separation [3, 4]. Nowadays, the preparation of highly selective and easy-separated 1-hexene and 1-octene by ethylene trimerization and tetramerization can enhance raw material usage and minimize manufacturing costs, which has piqued the interest of the industrial sphere [5].

Nowadays, continuous production has been proved to be more efficient and reliable than intermittent production in the organic chemical industry [6]. Michael et al. researched the catalytic behavior of NiMCM-41 in a continuous stirred tank reactor (CSTR), and NiMCM-41 is easily inactivated above 70 °C [7]. Xu et al. reported that ethylene oligomerization reactions over CoOx/N–C were highly selective to linear α-olefins at 80 °C in continuous flow reactors but only 5.2% 1-octene at 20% conversion [8, 9]. Finiels et al. reported that Ni-sulfated alumina (1.7 wt% Ni) catalyzed ethylene oligomerization and revealed high activity and stability against deactivation at low temperature and pressure in a continuous slurry reactor [10]. The majority of continuous reactions employ metal catalytic systems such as nickel and cobalt, but the continuous reaction of ethylene oligomerization catalyzed by metal chromium has received less attention. Kuhlman et al. reported the ethylene tri/tetramerization catalyzed by Cr(III)/DMP-PNP/MMAO carried out only in a push flow tubular reactor (PFTR) [11]. There have been no studies on homogeneous silicon-bridged diphosphines/chromium complexes (PNSiP/Cr) catalyzed ethylene oligomerization for CSTR thus far.

Our group developed a series of PNSiP/Cr used in catalyzing intermittent ethylene tri- and tetramerization with high catalytic activity and product selectivity [12–15]. Here we aimed to further evaluate the PNSiP/$CrCl_3(THF)_3$/MMAO catalytic systems for continuous ethylene tri-/tetramerization in CSTR. We have also conducted kinetic studies to determine the reaction order of chromium concentration and ethylene pressure relative to ethylene tri-/tetramerization, and finally calculated the apparent activation energy and rate equation to provide basic data for industrial production.

Experimental and methods

CSTR pilot design

All catalyst preparation procedures are completed in an oxygen-free environment, with purified and dried cyclohexane as solvent (Dehydration and drying with a 4A molecular sieve). PNSiP/$CrCl_3(THF)_3$ complex (Fig. 1) and MMAO as an activator make up the catalytic system. Akzo Nobel and Strom contributed MMAO and chromium precursors, respectively. In prior studies, we have already developed and synthesized the PNSiP/$CrCl_3(THF)_3$ complex [15].

Fig. 2 shows the flow chart of continuous ethylene tri-/tetramerization in CSTR. The main components include catalyst tank (3 L), cocatalyst tank (3 L), solvent feeder (5 L), CSTR (1 L), oligomers storage tank (10 L), temperature controller, pressure transducer, vacuum system, gas generation system, gas chromatography and flame ionization detection (GC-FID). CSTR is made up of a stainless container, two pairs of high-speed three-bladed electromechanical agitators, a liquid level indicator, and a heat exchange jacket. The temperature of CSTR is regulated by a temperature indicator controller (TIC) temperature controller and monitored by thermocouples. The ethylene and nitrogen are supplied into CSTR through the top pipe, where the differential pressure gauge and pressure indicator controller (PID) control the pressure. A high-performance liquid chromatography (HPLC) type pump controls the liquid flow when the solvent is utilized. A discharge valve and pipeline are located at the bottom of the catalyst and cocatalyst tanks. The overflow pipeline attached to CSTR is constructed with a 60° inclination angle to avoid the polyethylene (PE) solid phase in the reaction

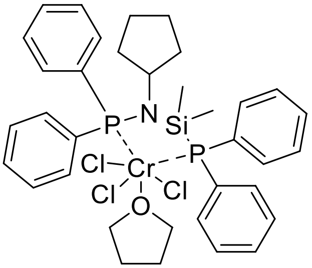

Fig. 1 Molecular structure of PNSiP/$CrCl_3(THF)_3$ complex [15]

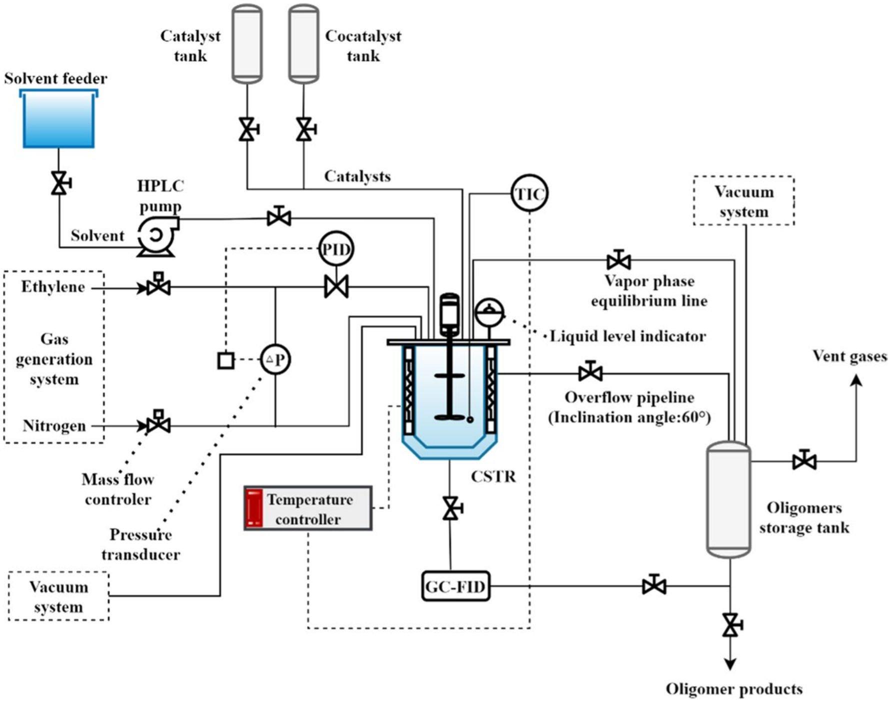

Fig. 2 Flow chart of continuous ethylene tri-/tetramerization in CSTR

product from clogging the overflow pipeline, ensuring long-term stable operation of the continuous ethylene tri-/tetramerization.

Continuous ethylene tri-/tetramerization reaction

The catalytic system (PNSiP/$CrCl_3(THF)_3$/MMAO) was suspended in liquid solvent cyclohexane at a preset stirring speed during ethylene tri-/tetramerization at the required pressure and temperature. Before each experiment, high-purity nitrogen (99.99%) and high-purity ethylene (99.99%) are first introduced to pump and clean the device multiple times, and then the heat exchange jacket is preheated to the preset temperature using the temperature control system to make the catalyst thermally activated in CSTR. According to the predetermined feed rate, the solvent, PNSiP/$CrCl_3(THF)_3$ complex, and MMAO were progressively supplied into CSTR for ethylene tri-/tetramerization. The liquid phase product was collected via the bottom of the CSTR, and the liquid phase components were quantitatively analyzed using GC-FID. With *n*-heptane as the internal standard, we calculate the catalytic activity of the product in ethylene tri-/tetramerization.

$$\text{Activity} = \frac{\mathrm{f} \times \mathrm{m_s} \times \mathrm{A_i} \times \mathrm{Wt} \times 10^6}{\mathrm{t} \times \mathrm{A_s} \times \mathrm{m_i} \times \mathrm{n(Cr)} \times 52} \tag{1}$$

Here f is a mass correction factor; m_s is the mass of *n*-heptane, g; m_i is the mass of product extracted, g; Wt is the mass of the product, g; A_s is the peak area of *n*-heptane; A_i is the peak area of product extracted; t is the reaction time, h; n(Cr) is the moles of metal catalyst activity center, μmol.

The yield of PE was examined by weighing the solid phase after vacuum drying.

Results and discussion

Effects of reaction temperature on ethylene tri-/tetramerization in CSTR

Table 1 shows the catalytic activity and selectivity of the PNSiP/$CrCl_3(THF)_3$/MMAO system in CSTR as the reaction temperature varies from 40 to 80 °C. The activity rose with the reaction temperature initially, peaking at a maximum (8.11×10^5 g(products) $g(Cr)^{-1}$ h^{-1}) at 60 °C before declining somewhat. The initial enhancement of catalytic activity is due to the increase of average kinetic energy at high temperatures. However, higher temperatures may result in reduced ethylene concentrations in cyclohexane and deactivation of the active center, reducing catalytic activity 14. The trend of the total selectivity of 1-hexene and 1-octene is consistent with that of activity, and also reaches a maximum (89.45%) at 60 °C. This may be because the chain growth rate of the active center in ethylene tri-/tetramerization increases faster than the chain transfer rate as the reaction temperature rises from 40 to 60 °C 13. Excessive metal active centers are inactivated when the reaction temperature surpasses 60 °C, which is detrimental to improving the total selectivity of 1-hexene and 1-octene. The selectivity of the C_{10+} products increased with reaction temperature, owing to the continuous participation of 1-butene, 1-hexene, and 1-octene in the secondary reaction at high temperatures. As a result, in CSTR,

Table 1 Effects of reaction temperature on catalytic activity and product selectivity in CSTR

T (°C)	Activity (10^5 g(products) $g(Cr)^{-1}$ h^{-1})	Product selectivity (wt%)						
		$C_4{}^a$	$1-C_4{}^b$	$C_6{}^a$	$C_8{}^a$	$C_{10+}{}^a$	$1-C_6{}^c+1-C_8{}^d$	cy-$C_6{}^e$
40	2.42	0.93	0.60	34.55	55.52	8.18	88.40	0.82
50	6.63	0.90	0.63	34.58	54.76	8.91	89.02	0.85
60	8.11	0.89	0.58	33.91	56.89	7.35	89.45	0.96
70	7.75	0.85	0.68	35.99	53.08	9.27	88.02	0.81
80	6.92	0.96	0.75	36.96	51.27	10.04	86.42	0.77

General conditions: *n*(Cr), 2.0 μmol; ethylene pressure, 5.0 MPa; solve, cyclohexane (200 mL); reaction time, 60 min; *n*(Al)/*n*(Cr), 466 equiv; *n*(ligand)/*n*(Cr), 1.05 equiv; impeller speed, 200 r/min; catalyst feed rate: 1.2 mL/min; cocatalyst, MMAO

[a] Mass fraction of butene, hexene, octene, decene and above α-olefins in liquid products

[b] Mass fraction of 1-butene in butane

[c] Mass fraction of 1-hexene in hexane

[d] Mass fraction of 1-octene in octane

[e] Mass fraction of methyl-cyclopentane and methylene-cyclopentane in liquid products

the PNSiP/$CrCl_3(THF)_3$/MMAO system has the highest reaction activity and total selectivity of 1-hexene and 1-octene at 60 °C.

Effects of ethylene pressure on ethylene tri-/tetramerization in CSTR

Table 2 shows the catalytic activity and selectivity of the PNSiP/$CrCl_3(THF)_3$/MMAO system with ethylene pressure changing from 1.0 to 6.0 MPa. The catalytic activity rises with increasing ethylene pressure, peaking at a maximum (87.50×10^4 g(products) $g(Cr)^{-1}$ h^{-1}) at 6.0 MPa. Because the solubility of ethylene monomer in the solvent increases as the reaction pressure rises, so does the diffusion rate of active center molecules, resulting in dramatically increased catalytic activity [16]. The total selectivity of 1-hexene and 1-octene reaches a maximum of 88.58% at 5.0 MPa, while the selectivities of Cyclic-C_6 and 1-butene are both less than 1.00% at 5.0 MPa. At 6.0 MPa, the selectivity of C_{10+} product is 10.69%, which is compatible with the results of high carbon product formation [17]. As a result, at 5.0 MPa, the PNSiP/$CrCl_3(THF)_3$/MMAO system demonstrates the greatest activity and total selectivity of 1-hexene and 1-octene selectivity in CSTR.

Effects of catalyst feed rate on ethylene tri-/tetramerization in CSTR

Table 3 shows the catalytic activity and selectivity of the PNSiP/$CrCl_3(THF)_3$/MMAO system. The activity of the catalyst rose first and subsequently declined with the catalyst feed rate raised from 0.25 to 3.00 mL/min. When the feed rate of the catalyst is too low, the contact time between the main catalyst and the cocatalyst

Table 2 Effects of ethylene pressure on catalytic activity and product selectivity in CSTR

P^a (MPa)	Activity (10^4 g(products) $g(Cr)^{-1}$ h^{-1})	Product selectivity (wt%)						
		$C_4{}^b$	$1-C_4{}^c$	$C_6{}^b$	$C_8{}^b$	$C_{10+}{}^b$	$1-C_6{}^d+1-C_8{}^e$	cy-$C_6{}^f$
1.0	3.09	0.79	0.66	49.85	40.57	7.59	87.08	1.20
2.0	6.73	0.66	0.58	47.98	41.58	8.25	88.17	1.53
3.0	11.23	0.53	0.37	46.15	42.81	9.12	87.46	1.39
4.0	29.03	0.48	0.39	39.71	49.1	9.11	88.06	1.60
5.0	87.11	0.51	0.43	35.57	54.43	8.56	88.58	0.93
6.0	87.50	0.79	0.66	32.88	54.61	10.69	86.26	1.03

General conditions: *n*(Cr), 2.0 μmol; *T*, 60 °C; solve, cyclohexane (200 mL); reaction time, 60 min; *n*(Al)/*n*(Cr), 466 equiv; *n*(ligand)/*n*(Cr), 1.05 equiv; impeller speed, 200 r/min; catalyst feed rate: 1.2 mL/min; cocatalyst, MMAO

[a] Ethylene pressure

[b] Mass fraction of butene, hexene, octene, decene and above α-olefins in liquid products

[c] Mass fraction of 1-butene in butane

[d] Mass fraction of 1-hexene in hexane

[e] Mass fraction of 1-octene in octane

[f] Mass fraction of methyl-cyclopentane and methylene-cyclopentane in liquid products

Table 3 Effects of catalyst feed rate on catalytic activity and product selectivity in CSTR

f^a (mL/min)	n(Cr) (μmol)	Activity (10^4 g(products) g(Cr)$^{-1}$ h^{-1})	Product selectivity (wt%)						
			C_4^{b}	$1-C_4$^{c}	C_6^{b}	C_8^{b}	C_{10+}^{b}	$1-C_6^{d}+1-C_8$^{e}	cy-C_6^{f}
0.25	0.42	6.86	6.95	5.88	33.51	50.44	8.02	82.21	1.08
0.50	0.83	11.11	2.57	1.49	34.72	52.60	9.28	86.53	0.83
1.00	1.67	30.96	1.36	1.29	36.84	51.73	9.26	87.94	0.81
1.20	2.00	63.46	0.35	0.22	36.79	52.69	9.36	88.99	0.81
1.50	2.50	60.57	0.85	0.74	36.34	51.88	10.18	87.10	0.75
2.00	3.33	42.88	0.62	0.51	37.73	50.63	10.28	86.79	0.74
3.00	5.00	34.23	0.50	0.42	38.83	48.55	11.31	86.45	0.81

General conditions: T, 60 °C; ethylene pressure, 5.0 MPa; solve, cyclohexane (200 mL); reaction time, 60 min; n(Al)/n(Cr), 466 equiv; n(ligand)/n(Cr), 1.05 equiv; impeller speed, 200 r/min; cocatalyst, MMAO

[a] Catalyst feed rate

[b] Mass fraction of butene, hexene, octene, decene and above α-olefins in liquid products

[c] Mass fraction of 1-butene in butane

[d] Mass fraction of 1-hexene in hexane

[e] Mass fraction of 1-octene in octane

[f] Mass fraction of methyl-cyclopentane and methylene-cyclopentane in liquid products

Table 4 Effects of impeller speed on catalytic activity and product selectivity in CSTR

Speed (r/min)	Activity (10^5 g(products) $g(Cr)^{-1}$ h^{-1})	Product selectivity (wt%)						
		C_4[a]	$1-C_4$[b]	C_6[a]	C_8[a]	C_{10+}[a]	$1-C_6$[c]$+1-C_8$[d]	cy-C_6[e]
100	4.30	0.37	0.26	35.46	53.41	9.93	88.53	0.83
200	6.34	0.35	0.22	36.79	52.69	9.36	88.99	0.81
250	6.46	0.38	0.29	35.87	51.93	10.98	87.58	0.84
300	6.86	0.41	0.33	31.70	53.48	13.52	84.52	0.89
310	6.78	0.39	0.31	31.81	52.99	13.88	84.36	0.93
320	6.81	0.56	0.41	32.61	52.28	13.67	83.96	0.88
350	6.80	0.45	0.38	31.96	52.72	13.97	84.13	0.90

General conditions: *n*(Cr), 2.0 μmol; *T*, 60 °C; ethylene pressure, 5.0 MPa; solve, cyclohexane (200 mL); reaction time, 60 min; *n*(Al)/*n*(Cr), 466 equiv; *n*(ligand)/*n*(Cr), 1.05 equiv; catalyst feed rate, 1.20 mL/min; cocatalyst, MMAO

[a] Mass fraction of butene, hexene, octene, decene and above α-olefins in liquid products

[b] Mass fraction of 1-butene in butane

[c] Mass fraction of 1-hexene in hexane

[d] Mass fraction of 1-octene in octane

[e] Mass fraction of methyl-cyclopentane and methylene-cyclopentane in liquid products

is too long under olefin-free conditions, resulting in over alkylation and deactivation of the catalyst; when the feed rate is too high, most of the chromium complex cannot coordinate with ethylene in time and fails to form active center [18]. As a result, when the catalyst feed rate is 1.20 mL/min, the total selectivity of the 1-hexene and 1-octene reaches the maximum (88.99%) and the catalytic activity is highest (63.46×10^4 g(products) $g(Cr)^{-1}$ h^{-1}) in CSTR.

Effects of impeller speed on ethylene tri-/tetramerization in CSTR

Table 4 shows the catalytic activity and selectivity of the PNSiP/$CrCl_3(THF)_3$/MMAO system with impeller speed changing from 100 to 320 r/min. The catalytic activity increases with impeller speed, peaking at 6.86×10^5 g(products) $g(Cr)^{-1}$ h^{-1} at 300 r/min. The following factors can be related to the enhancement of catalytic activity: On the one hand, high impeller speed enhances ethylene solubility in cyclohexane solvent; on the other hand, high impeller speed increases the contact frequency between ethylene and chromium catalyst active center species. At 300 r/min, the total selectivity of 1-hexene and 1-octene declined while the selectivity of C_{10+} rose, and this is due to the higher contact probability of the secondary reactions of 1-butene, 1-hexene, and 1-octene to C_{10+} products [19]. When the impeller speed exceeds 300 r/min, the activity and product selectivity tend to be stable, and the effect of mass transfer resistance between the liquid phase and solid phase can be ignored. Therefore, from a comprehensive point of view, we set the impeller speed of CSTR to 200 r/min.

Table 5 Effects of running time on catalytic activity and product selectivity in CSTR

Running time (h)	Activity (10^5 g(products) g(Cr)$^{-1}$ h^{-1})	Product selectivity (wt%)						
		C_4[a]	$1-C_4$[b]	C_6[a]	C_8[a]	C_{10+}[a]	$1-C_6$[c]$+1-C_8$[d]	cy-C_6[e]
1	6.26	0.71	0.62	36.37	53.36	8.74	89.23	0.82
2	6.36	0.83	0.72	36.77	53.07	8.49	89.36	0.84
3	6.42	0.54	0.45	36.35	53.62	8.66	89.49	0.83
4	6.86	0.81	0.72	37.17	51.66	9.53	88.27	0.83
5	6.71	0.76	0.63	39.38	50.65	8.40	89.45	0.81
6	6.71	0.77	0.62	37.80	50.68	9.95	87.92	0.80
7	6.88	0.69	0.56	37.79	50.94	9.80	88.14	0.78
8	6.36	0.56	0.41	37.99	50.07	10.59	87.56	0.79
9	6.69	0.79	0.6	37.48	51.64	9.27	88.61	0.82
10	6.44	0.35	0.22	36.79	52.69	9.36	88.99	0.81
11	6.84	0.24	0.13	37.08	52.28	9.60	88.87	0.80
12	6.71	0.47	0.25	38.48	51.02	9.28	88.82	0.75
13	6.36	0.69	0.50	39.13	50.08	9.26	88.65	0.84
14	6.61	0.77	0.59	38.78	50.36	9.3	88.57	0.79
15	7.26	0.33	0.19	36.67	52.43	9.82	88.51	0.75
16	6.42	0.30	0.16	38.07	50.78	10.06	88.33	0.79
17	6.84	0.32	0.24	36.19	51.31	11.38	87.20	0.80
18	6.38	0.27	0.19	36.85	51.64	10.44	88.22	0.80
19	7.09	0.27	0.19	36.23	51.21	11.54	87.18	0.75
20	6.71	0.25	0.16	37.79	51.02	10.18	88.48	0.76
21	6.00	0.19	0.12	38.24	50.50	10.21	88.49	0.86
22	7.09	0.29	0.19	37.15	51.01	10.70	87.80	0.85
23	7.21	0.36	0.22	37.51	50.52	10.75	87.62	0.86
24	7.03	0.57	0.41	39.91	48.57	10.16	87.91	0.79
25	7.15	0.56	0.41	41.15	46.98	10.54	87.49	0.77
26	7.03	0.63	0.41	42.61	45.23	10.77	87.14	0.76
27	6.48	0.59	0.38	43.09	44.38	11.19	86.72	0.75
28	7.30	1.04	0.78	44.18	43.18	10.84	86.53	0.76
29	6.82	0.53	0.30	45.47	42.48	10.77	87.06	0.75
30	6.46	0.56	0.35	49.45	37.83	11.46	86.09	0.70

General conditions: *n*(Cr), 2.0 µmol; *T*, 60 °C; ethylene pressure, 5.0 MPa; solve, cyclohexane (200 mL); *n*(Al)/*n*(Cr), 466 equiv; *n*(ligand)/*n*(Cr), 1.05 equiv; impeller speed, 200 r/min; catalyst feed rate, 1.20 mL/min; cocatalyst, MMAO

[a] Mass fraction of butene, hexene, octene, decene and above α-olefins in liquid products

[b] Mass fraction of 1-butene in butane

[c] Mass fraction of 1-hexene in hexane

[d] Mass fraction of 1-octene in octane

[e] Mass fraction of methyl-cyclopentane and methylene-cyclopentane in liquid products

Effects of running time on ethylene tri-/tetramerization in CSTR

Table 5 shows the catalytic activity and selectivity of the PNSiP/$CrCl_3(THF)_3$/MMAO system with the running time changing from 1 to 30 h. We measured the catalytic activity and product selectivity of the catalyst in the tank every hour. During the long-term operation of CSTR for 30 h, the catalytic activity remained over 6.00×10^5 g(products) $g(Cr)^{-1}$ h^{-1}, and the total selectivity of 1-hexene and 1-octene was greater than 86.09% with no notable variation. The PE mass fraction (including PE overflowing into the product storage tank) in the CSTR reaction product is just 0.15% after 30 h, indicating that CSTR can efficiently limit PE accumulation, ensuring the continuous and stable reaction. Furthermore, the selectivity of Cyclic-C_6 is less than 1.00%, indicating that the disproportionation reaction of metal chromium cycloheptane in CSTR is insignificant. Due to the relatively high average product concentration in the reaction solution, a minor quantity of C_{10+} will be generated in the latter stages of such reactions in CSTR 14.

Kinetic investigation—effects of chromium concentration

According to the above study, we further assessed the kinetic parameters of the reaction system in CSTR and utilized the initial rate method for the development of the following kinetic equation (Eq. 2) [20, 21]

$$v_a = k[C]^m[M]^n \tag{2}$$

The reaction rates of reactions conducted were obtained from the GC data of samples taken throughout these reactions. In different catalytic systems, the kinetic reaction order of the catalytic process differs. As far as we know, the reaction rate

Table 6 Effects of chromium concentration on v_a in CSTR

Entry	Chromium concentration (μmol/L)	$v_a{}^a$ (g(products) h^{-1})
1	1.77	20.54
2	3.55	40.88
3	4.25	55.92
4	5.31	64.70
5	7.09	92.24
6	9.21	65.56
7	11.34	45.72
8	13.66	25.70
9	20.00	12.50

General conditions: *T*, 60 °C; ethylene pressure, 5.0 MPa; solve, cyclohexane (200 mL); *n*(Al)/*n*(Cr), 466 equiv; *n*(ligand)/*n*(Cr), 1.05 equiv; impeller speed, 200 r/min; cocatalyst, MMAO

[a] Reaction rate is only based on the reaction rate of liquid products

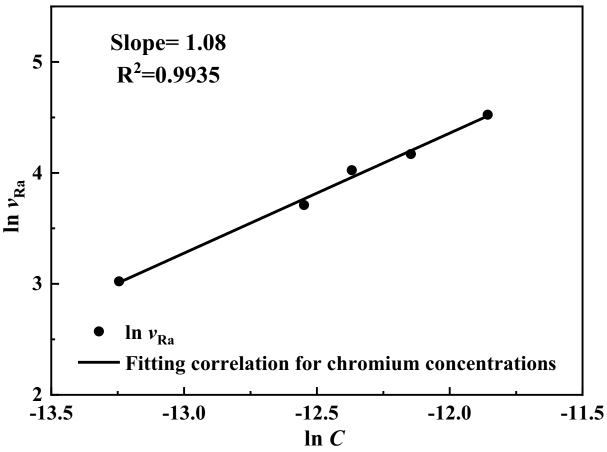

Fig. 3 Dependence of reaction rate on chromium concentration in CSTR. General conditions: *T*, 60 °C; ethylene pressure, 5.0 MPa; *n*(Al)/*n*(Cr), 466 equiv; *n*(ligand)/*n*(Cr), 1.05 equiv; impeller speed, 200 r/min; cocatalyst, MMAO

dependence on ethylene concentration in the intermittent reaction kinetics of ethylene oligomerization is in the order of 1–1.95, and the reaction rate dependence on catalyst concentration is in the order of 0.6–1.12 [22–25].

Table 6 shows the changing of reaction rate v_a with chromium concentration at the ethylene pressure of 5.0 MPa. According to Jan's report, the ethylene solubility in the solvent, which strongly depends on pressure, is an important property for ethylene oligomerization [26]. In the range of temperature and ethylene pressure

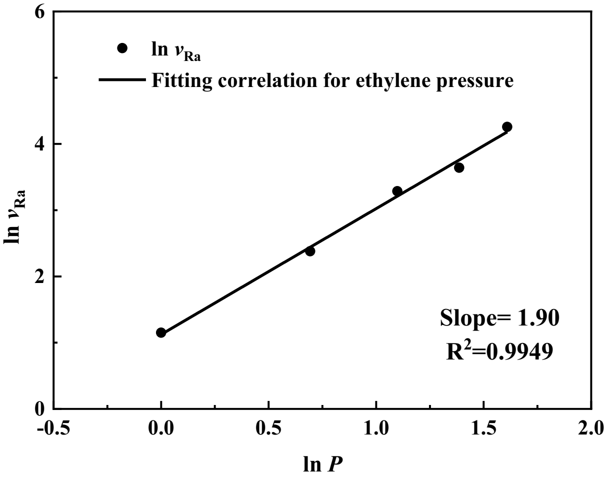

Fig. 4 Dependence of total products formation rate on ethylene pressure in CSTR. General conditions: *T*, 60 °C; n(Cat), 2 μmol; *n*(Al)/*n*(Cr), 466 equiv; *n*(ligand)/*n*(Cr), 1.05 equiv; impeller speed, 200 r/min; cocatalyst, MMAO

studied, the solubility of ethylene and ethylene pressure conform to Henry's law [27–29]. According to the previous Ruta's report, under the condition of fixed ethylene pressure, we can ignore the changes in ethylene solubility, and the liquid phase is at a relatively low level in this reaction [30]. The reaction order with respect to chromium concentration could now be determined from the relationship of a ln v_a versus ln C. The reaction order of chromium concentration on ethylene tri-/tetramerization is 1.08 (Fig. 3), indicating that chromium active sites are involved in the catalytic process. The catalytic activity of the system was enhanced when the chromium concentration was raised from 1.77 to 7.09 μmol/L, and it was lowered when the chromium concentration exceeded 7.09 μmol/L. This alteration might be related to the synthesis of chromium trimers of inactive species at high chromium concentration, as previously reported [31].

Kinetic investigation—effects of ethylene pressure

Within the range of reaction temperature and ethylene pressure understudy, the solubility of ethylene in cyclohexane is proportional to the ethylene pressure conformed to Henry's law [27–29]. Therefore, the ethylene pressure p can be directly correlated with the reaction rate v_a, and the expression of Eq. 1 is simplified to Eq. 3:

$$\mathrm{v_a = k[C]^m P^{\,n}} \tag{3}$$

The reaction order with respect to chromium concentration could now be determined from the relationship of a ln v_a versus ln P. Fig. 4 shows the linear fitting results derived in the pressure range of 1.0 MPa to 5.0 MPa. The reaction order of ethylene concentration is 1.90 on ethylene tri-/tetramerization in CSTR, which is consistent with prior reports [32].

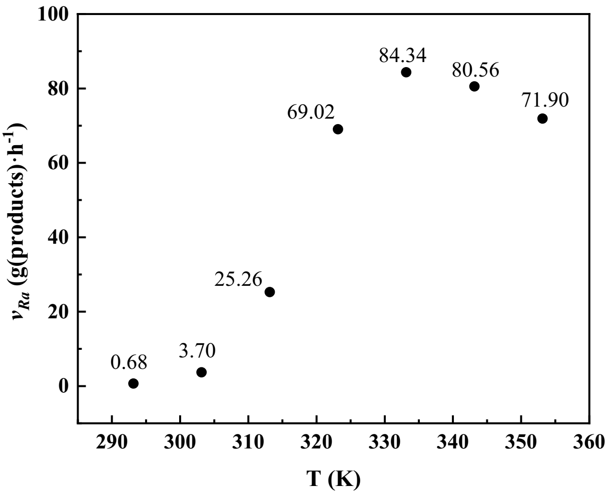

Fig. 5 Change trend between reaction rate and reaction temperature in CSTR

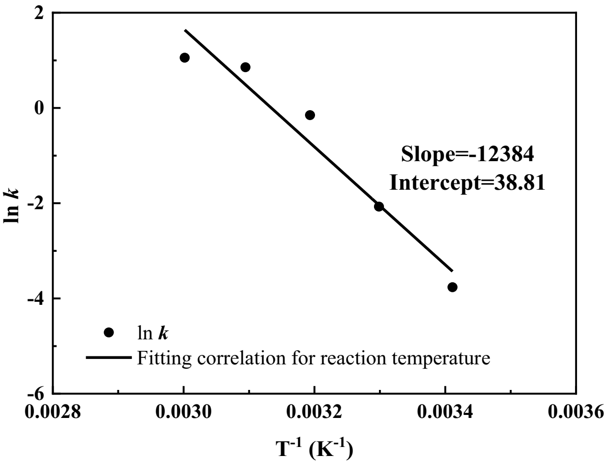

Fig. 6 Relationship between reaction rate constant and reaction temperature in CSTR. General conditions: *C*(Cat), 7.09 μmol/L; ethylene pressure, 5.0 MPa; *n*(Al)/*n*(Cr), 466 equiv; *n*(ligand)/*n*(Cr), 1.05 equiv; impeller speed, 200 r/min; cocatalyst, MMAO

Determination of kinetic parameters—temperature dependence

We researched the reaction state increasing from 293.15 to 353.15 K at 5.0 MPa to determine the influence of reaction temperature on reaction rate. The Arrhenius equation (Eq. 4) and the logarithmic calculation equation (Eq. 5) will be used to discuss the following part [32].

$$\mathrm{k} = \mathrm{A} \times \mathrm{e}^{\frac{-\mathrm{E_a}}{\mathrm{RT}}} \tag{4}$$

$$\ln \mathrm{k} = -\frac{\mathrm{E_a}}{\mathrm{RT}} + \ln \mathrm{A} \tag{5}$$

Here A is the Arrhenius constant; E_a is the apparent activation energy, J/mol; R is the molar gas constant, J/(mol K); T is the absolute temperature, K.

We computed the reaction rate constant k at different temperatures (293.15 K to 353.15 K) using Eq. 4 by combining the reaction order obtained earlier. In the case of the Arrhenius diagram, we can find that the reaction rate is heavily influenced by reaction temperature and exhibits two distinct states at 5.0 MPa (Figs. 5 and 6): (a) From 293.15 K to 333.15 K, the reaction rate the temperature is essentially linear; (b) From 333.15 K to 353.15 K, the reaction rate falls dramatically as the temperature rises and there is no linear relationship, which is consistent with a previous report [22].

The slope of the straight line in the temperature from 293.15 to 333.15 K is − 12,384 (Fig. 6), and the activation energy of ethylene tri-/tetramerization in CSTR is 102.96 kJ/mol. The homogeneous catalytic reaction under this activation energy is consistent with a previous report [31]. Equations (3) and (4) can be combined to form Eq. 6. We then get the rate equation of ethylene tri-/tetramerization (Eq. 7) from 293.15 to 333.15 K in CSTR using Eq. 6 of reaction rate:

$$\mathrm{v_a} = A \times \mathrm{e}^{\frac{-\mathrm{E_a}}{\mathrm{RT}}}[\mathrm{C}]^{\mathrm{m}}[\mathrm{p}]^{\mathrm{n}} \tag{6}$$

$$\mathrm{v_a} = 7.17 \times 10^{16} \times \exp\left(-\frac{102960}{\mathrm{RT}}\right)\mathrm{C}^{1.08}\mathrm{p}^{1.90} \tag{7}$$

Conclusion

In conclusion, the optimum process parameters for continuous ethylene tri-/tetramerization in CSTR based on PNSiP/$CrCl_3(THF)_3$/MMAO system are as follows: The reaction temperature is 60 °C; the ethylene pressure is 5.0 MPa; the catalyst feed rate is 1.20 mL/min; the impeller speed is 200 r/min. Over the 30 h of reaction, the activity and product selectivity were consistently balanced within 7.26×10^5 g(products) $g(Cr)^{-1}$ h^{-1} and 88%. The reaction order of chromium concentration on ethylene tri-/tetramerization is 1.08, and the reaction order to ethylene pressure is 1.90. When the chromium concentration is 7.09 µmol/L, the temperature is 20 °C to 60 °C, and the ethylene pressure is 5.0 MPa, the apparent activation energy of the reaction is 102.96 kJ/mol. In summary, the preparation of linear α-olefins by CSTR under the best conditions provides a promising choice for pilot and industrial production in the future.

Acknowledgements This research was sponsored by the financial support from the National Natural Science Foundation of China (NSFC) (Grant Nos. 22071178, 22050410271), the Natural Science Foundation of Hebei Province of China (Grant No. B2019109045), China Petroleum Science and technology program (Grant No. 2020B-2512) and PetroChina Innovation Foundation (Grant No. 2020D-5007-0405).

References

1. Dixon JT, Green MJ, Hess FM, Morgan DH (2004) J Organomet Chem 689:3641–3668
2. Kumar S, Dholakiya BZ, Jangir R (2021) J Organomet Chem 953:122066
3. Britovsek GJP, Malinowski R, McGuinness DS, Nobbs JD, Tomov AK, Wadsley AW, Young CT (2015) ACS Catal 5:6922–6925
4. Sheng D, Zhang Y, Wang Z, Xu G, Song QX, Shan DM, Hou HQ (2021) J Organomet Chem 956:122128
5. Kim Y, Jung U, Song D, Im HB, Park JC, Youn MH, Jeong HD, Rhim GB, Chun DH, Lee DW, Lee KB, Koo KY (2020) Fuel 281:118791
6. Sydora OL (2019) Organometallics 38:997–1010
7. Lallemand M, Finiels A, Fajula F, Hulea V (2011) Chem Eng J 172:1078–1082
8. Xu Z, Chada JP, Xu L, Zhao D, Rosenfeld DC, Rogers JL, Hermans I, Mavrikakis M, Huber GW (2018) ACS Catal 8:2488
9. Xu Z, Zhao D, Chada JP, Rosenfeld DC, Rogers JL, Hermans I, Huber GW (2017) J Catal 354:213–222
10. Finiels A, Fajula F, Hulea V (2014) Catal Sci Technol 4:2412–2426
11. Kuhlmann S, Paetz C, Hägele C, Blann K, Walsh R, Dixon JT, Scholz J, Haumann M, Wasserscheid PJ (2009) J Catal 262:83–91

12. Alam F, Zhang L, Zhai Y, Wang J, Tang H, Chen Y, Jiang T (2019) J Catal 378:312–319
13. Alam F, Wang J, Dong C, Chang Q, Zhang L, Zhang Q, Chen Y, Jiang T (2020) J Catal 392:278–286
14. Alam F, Zhang L, Wei W, Wang J, Chen Y, Dong C, Jiang T (2018) ACS Catal 8:10836–10845
15. Zhang L, Wei W, Alam F, Chen Y, Jiang T (2017) Catal Sci Technol 7:5011–5018
16. Jiang T, Ning Y, Zhang B, Li J, Wang G, Yi J, Huang Q (2006) J Mol Catal A 259:161–165
17. Wang J, Shang Y, Zhang N, Li C, Shi W (2018) Russ J Phys Chem 92:2618–2627
18. Do LH, Labinger JA, Bercaw JE (2013) ACS Catal 3:2582–2585
19. Zhang J, Alam F, Fan H, Ma J, Jiang T (2022) Appl Organomet Chem 36:e6454
20. Mohammed AA, Fateen S, Ahmed TS, Moustafa TM (2014) Appl Petrochem Res 4:287–295
21. Lente G (2015) Deterministic kinetics in chemistry and systems biology: the dynamics of complex reaction networks. Springer, New York
22. Walsh R, Morgan DH, Bollmann A, Dixon JT (2006) Appl Catal A 306:184–191
23. Kuhlmann S, Dixon JT, Haumann M, Morgan DH, Ofili J, Spuhl O, Taccardi N, Wasserscheid P (2006) Adv Synth Catal 348:1200–1206
24. Tang S, Liu Z, Yan X, Li N, Cheng R, He X, Liu B (2014) Appl Catal A 481:39–48
25. Hagen H (2006) Ind Eng Chem Res 45:3544–3551
26. Jan O, Song K, Dichiara A, Fernando LP (2018) Ind Eng Chem Res 57:10241–10250
27. Kishor R, Padmanabhan S (2011) R Sarma K, Patel V, Sharma S, Parimal AP. J Appl Poly Sci 122:2646–2652
28. Shaharun MS, Mukhtar H, Dutta BK (2008) Chem Eng Sci 63:3024–3035
29. Coughlin RW, Pollak FA (1969) AIChE J 15:208–214
30. Ruta M, Laurenczy G, Dyson PJ, Kiwi-Minsker L (2008) J Phys Chem C 112:17814–17819
31. Kuhlmann S (2006) Universitat Erlangen-Nurnberg
32. Chen G, Liu H, Fadaeerayeni S, Shan J, Xing A, Cheng J, Wang H, Xiang Y (2020) Catal Sci Technol 10:4019–4029